

# Structure of Charged Dendrimer Solutions As Seen by Small-Angle Neutron Scattering

Giovanni Nisato,<sup>†</sup> Robert Ivkov, and Eric J. Amis\*

Polymers Division, National Institute of Standards and Technology, 100 Bureau Dr. Stop 8542, Gaithersburg, Maryland 20899-8542

Received April 22, 1999; Revised Manuscript Received June 24, 1999

**ABSTRACT:** We present results of small-angle neutron scattering (SANS) investigations into the characteristics of charged poly(amidoamine) (PAMAM) dendrimer solutions in deuterium oxide. The study shows that ionic strength, surface charge density, and concentration are the crucial parameters controlling the degree of structural organization of the solution. Upon the addition of acid, HCl, we observe a peak in the scattering intensity. The results indicate that increasing ionization of terminal amines results in interparticle interactions giving rise to local, liquidlike ordering. These interactions can be screened by adding monovalent salt (NaCl) in large quantities. The short-range interactions were studied by systematically varying dendrimer and salt concentration (up to 2 M). Contrary to most weak polyelectrolyte systems, we did not observe a negative second virial coefficient, even for the highest salt concentrations.

## Introduction

Dendrimers are highly branched macromolecules consisting of a multifunctional core from which successive branched repeat units extend radially outward. The resulting molecules have a well-defined number of end groups and narrow molecular weight distribution.<sup>1,2</sup> These molecules are synthesized in a stepwise manner so that each new step, or generation, doubles the molecular weight, the number of end groups, and the number of branch points. In addition, it was recently found that with successive generations dendrimers become increasingly spherical, their form factor evolving from starlike at low generation to dense sphere at higher generations.<sup>3</sup> The most frequently studied dendrimers contain amine-terminated end groups. In this case the surface charge densities of these molecules can be manipulated by varying the pH of the solution, and the dendrimers can be viewed as nanoscopic polyelectrolyte particles.

The nature of the interactions between macroions in solution has received considerable experimental and theoretical attention through the years.<sup>4</sup> Often, experimental efforts are directed toward a search for a suitable model system that allows direct comparison with theories. In general, model systems should consist of molecules with (1) uniform size and shape, (2) ionizable groups able to support large variations of charge density, and (3) solubility over a wide range of conditions to allow sampling a large parameter space. Dendrimers are good candidates for exploring the physics of macroions.

Aside from considerations of a theoretical nature, a number of potential applications for dendrimers, such as "smart" drug delivery agents, are expected to involve drastic changes in their aqueous environment. It is therefore important to assess the response of dendrimers to such changes. The goal of this study is to systematically vary the degree of ionization of the dendrimers as well as the ionic strength of the solution

in order to probe dendrimer–dendrimer interactions over a wide range of ionic conditions.

## Experimental Section

**Materials.** Generation 5 (G5) polyamidoamine (PAMAM) dendrimers were obtained from Dendritech, Inc., Midland, MI.<sup>5</sup> The G5 dendrimer solutions were prepared from a 0.22 mass fraction aqueous stock solution as follows. Aliquots of the stock solution were diluted with ultrapure H<sub>2</sub>O (18 MΩ/cm, Barnstead) and dialyzed to remove low molecular weight impurities. Dialysis was performed using a Spectrum microdialyzer with a 10 mL half-cell volume and a 12–14 kDa molecular weight cutoff (MWCO) cellulose membrane (Spectra/Por, Spectrum). H<sub>2</sub>O solvent was exchanged by dialysis against 99.9% (low paramagnetic) D<sub>2</sub>O (Cambridge Isotopes, Inc.).<sup>5,6</sup> The final D<sub>2</sub>O volume fraction of the solvent was >96.5%, as measured from the scattering intensity of the solution. The G5 PAMAM dendrimers have 128 terminal amine groups that can be ionized to the  $-NH_3^+$  form through the addition of a (strong) acid. The stoichiometric ratio of added HCl to the total number of terminal groups in solution is noted  $\alpha = [HCl]/[-NH_2]$ , and it is proportional, but does not correspond exactly, to the extent of the ionization of the terminal amine groups.

The values of dendrimer volume fraction,  $\phi$ , and  $\alpha$  were calculated from the weight of the added components and values of density, molecular weight, and functionality reported in the literature.<sup>7</sup> The main characteristics of the samples studied are listed in Tables 1–3.<sup>8</sup>

**SANS.** SANS data were obtained on the 8 and 30 m instruments located at the Center for Neutron Research at the National Institute of Standards and Technology in Gaithersburg, MD.<sup>9</sup> The 8 m measurements were performed using a sample-to-detector distance of 360 cm and an average neutron wavelength of 9 Å with a spread  $\Delta\lambda/\lambda = 0.25$ . These conditions yielded a  $q$  range of 0.008–0.123 Å<sup>-1</sup>, where  $q$  denotes the amplitude of the scattering vector. The 30 m SANS experiments were conducted using several detector configurations and 6 Å ( $\Delta\lambda/\lambda = 0.10$ ) neutrons, corresponding to a  $q$  range from 0.004 to 0.31 Å<sup>-1</sup>. All the samples were contained in quartz cells having circular windows and path lengths of 1, 2, or 5 mm. The raw (2-D) data were reduced following the standard data reduction software available at the Cold Neutron Research Facility.<sup>10</sup> The incoherent background level in the samples was estimated using two independent procedures. In the first one, a constant was subtracted so that the SANS data at high  $q$  values was adjusted to a  $q^{-4}$  slope in a log–log plot, following Glatter<sup>11</sup> and Chen.<sup>12</sup> In the cases when the data

\* Corresponding author.

<sup>†</sup> Current address: Philips Research, Prof. Holstlaan 4, NL-5656 AA Eindhoven, Netherlands.

**Table 1. Effect of Charge Density<sup>8</sup>**

sample	$\alpha$	$\phi \times 10^{-2}$	sample	$\alpha$	$\phi \times 10^{-2}$
d4-0-0	0.010	2.85	d4-0-3	0.221	2.79
d4-0-06	0.048	2.79	d4-0-5	0.449	2.79
d4-0-1	0.072	2.80	d4-0-10	0.960	2.790

**Table 2. Effect of Salt Concentration<sup>8</sup>**

sample	$\alpha$	$\phi \times 10^{-2}$	$C_s$ (M)
D1-0-5	0.57	0.61	0
D1-5-5	0.59	0.56	0.0050
D1-25-5	0.58	0.61	0.0250
D1-50-5	0.58	0.61	0.0500
D1-100-5	0.583	0.64	0.100
D1-1000-5	0.61	0.57	0.991

**Table 3. Effect of Dendrimer Concentration<sup>8</sup>**

sample	$\alpha$	$\phi \times 10^{-2}$	$q^*$ ( $\text{\AA}^{-1}$ )
D2-0-5	0.574	1.19	0.052
D1-0-5	0.574	0.61	0.044
D05-0-5	0.572	0.31	0.035
D02-0-5	0.574	0.11	0.025

at sufficiently high  $q$  was not available, the scattering profiles were fitted to a Guinier functional form with a floating baseline, which was shown by Prosa et al. to fit PAMAM dendrimers satisfactorily.<sup>3</sup> In the second procedure, the incoherent intensity was interpolated from the transmissions of the samples and the scattering intensities of known H<sub>2</sub>O and D<sub>2</sub>O mixtures.<sup>13</sup> In all cases, the resulting background corrections from these procedures were in good agreement (relative standard deviation <5%). The corrected intensities were then converted to an absolute scale and were radially averaged yielding the  $I$  vs  $q$  plots for each sample.<sup>10</sup> Experimental standard deviations in the scattered intensities were <1%, yielding uncertainty bars smaller than the plotted data symbols, and were not displayed for clarity.

The total scattering intensity  $I(q)$  from a homogeneous solution of monodispersed spherical particles can be written as<sup>14</sup>

$$I(q) = KP(q) S(q) \quad (1)$$

where  $K$  is the contrast factor,  $P(q)$  is the single particle form factor arising from intraparticle interference (Figure 1a), and  $S(q)$  is the solution structure factor corresponding to interparticle interference (Figure 1b). The contrast factor is proportional to the particle volume fraction and depends on the difference of scattering length densities between the particles and the solvent.<sup>14</sup> Expression 1 is exact in the case of spherical scattering objects and can be extended to the case of non-spherical particles by using an effective structure factor. The form factor corresponding to a given geometry and segment density distribution can be readily calculated.<sup>11,14</sup> The calculation of the structure factor  $S(q)$  in the case of charged colloids requires complex models describing the effects of the long-range Coulombic interactions.<sup>4</sup> Generally, when the particles interact, the changes in  $S(q)$  reflected in the overall scattering intensity arise from interparticle spatial correlations.<sup>11,14</sup> When  $q \gg R_g^{-1}$ , the structure factor is a constant  $S(q) = 1$ , and the total scattering reflects the nature of the individual particles (Figure 1b). The other interesting regime occurs when  $q \ll R_g^{-1}$ ; in this regime the scattering behavior is dominated by the osmotic compressibility of the solution. As  $q \rightarrow 0$ , the scattering intensity reduces to  $I(0) \sim k_B T(\partial\phi/\partial\Pi)_T \sim \phi(1 + A_2\phi)$ , where  $k_B$  is the Boltzmann constant,  $\Pi$  is the osmotic pressure of the solution, and  $A_2$  is the second virial coefficient.<sup>14</sup>

## Results and Discussion

In Figure 2 we display the excess scattering intensity of aqueous (D<sub>2</sub>O) dendrimer solutions prior to addition of salt or acid (i.e., in the preparation state) as a function of dendrimer concentration. The  $I(q)$  data are normal-

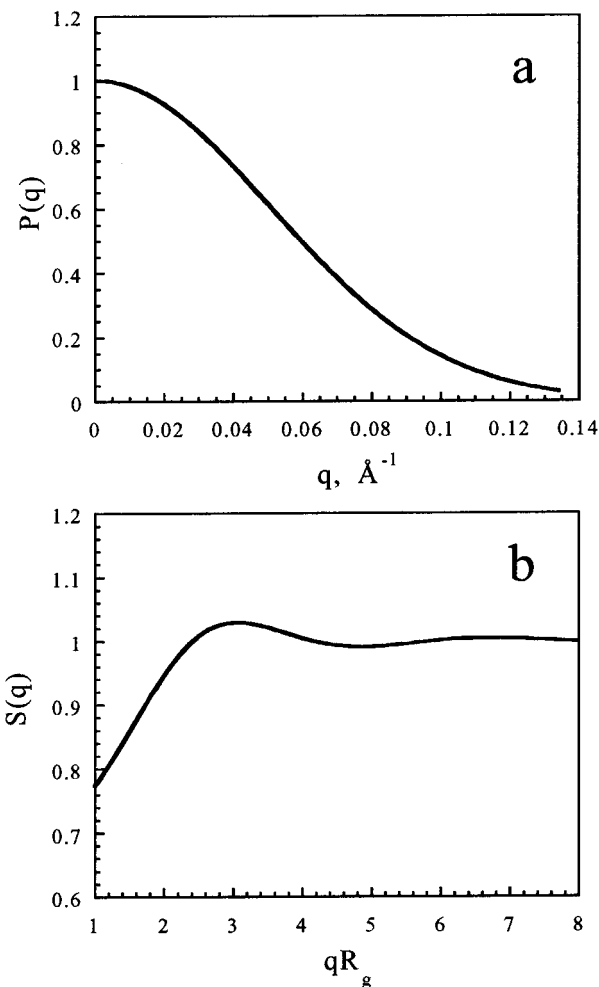


**Figure 1.** (a) Guinier functional form approximating the form factor  $P(q)$  of G5 PAMAM dendrimers.<sup>3</sup> (b) Example of structure factor  $S(q)$  of charged spherical colloids in suspension calculated using the RMSA approximation.<sup>4,27</sup>

ized by the overall dendrimer volume fraction, and a Guinier functional form  $I(q) = I_0 \exp(-q^2 R_g^2/3)$  could be satisfactorily fit to the data, independent of the dendrimer concentration, yielding the apparent radius of gyration of the molecules.<sup>3,15</sup> The value of the radius of gyration extrapolated at zero concentration from these measurement was  $24.3 \pm 0.5 \text{ \AA}$ ,<sup>16</sup> in agreement with previous SAXS experiments performed in methanol.<sup>3</sup> The concentration dependence of the apparent radius of gyration follows the same trend observed by Topp et al. in similar experiments performed on poly(propyleneimine) dendrimers.<sup>15</sup> We could also evaluate the (apparent) values of  $R_g$  in the case of charged dendrimer solutions in the presence of salt. The data reported in Figure 2b show that, for charged dendrimers with  $\alpha \approx 0.6$  and for salt concentrations ranging from 50 mM to 2 M,<sup>17</sup> we do not find significant variations of the radius of gyration. The influence of pH and salt concentration on the dendrimer size in dilute solution will be discussed in more detail in a forthcoming paper.<sup>18</sup>

Figure 3 shows the excess scattering profiles from solutions in which the dendrimer volume fraction was fixed at  $\phi \approx 0.042$  and  $\alpha$  was varied from 0.0 to 1.0 (one HCl per terminal unit or primary amine group). As the charge density of the dendrimers is increased by the addition of acid, the total osmotic pressure of the

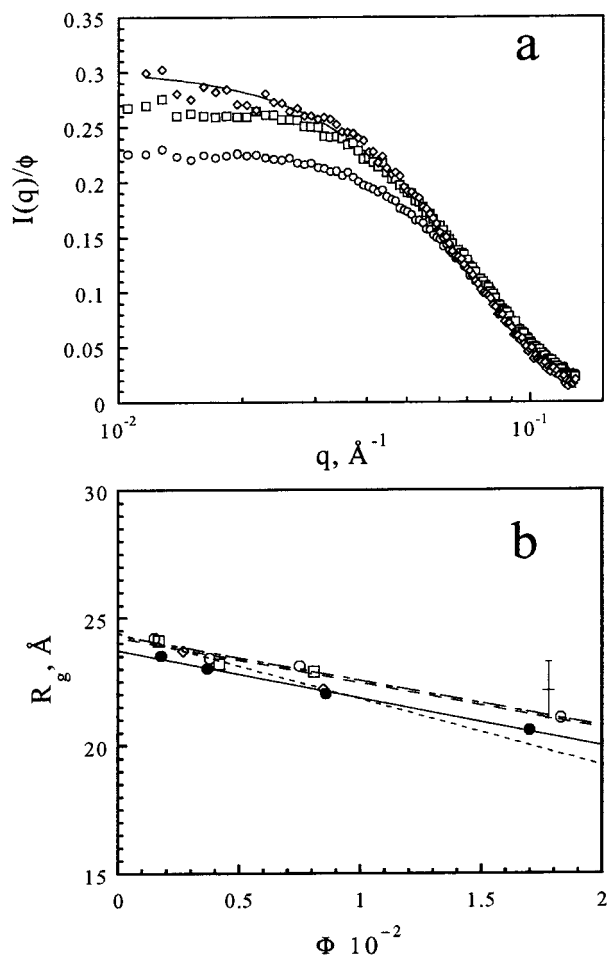


**Figure 2.** (a) Excess scattering from G5 PAMAM dendrimers. The data are normalized by the dendrimer volume fractions of the solutions, indicated in the legend. The solid line is a Guinier fit to the data.<sup>14</sup> (b) Volume fraction dependence of the apparent radius of gyration of PAMAM G5 dendrimers. The solid line is a linear fit to the data, yielding the radius of gyration extrapolated at zero concentration for  $\alpha = 0$  and no added salt (filled circles),  $\alpha = 0.6$  and  $C_S = 50$  mM (squares),  $C_S = 100$  mM (diamonds),  $C_S = 1000$  mM (circles), and  $C_S = 2000$  mM (cross). When not shown, the bars in all figures are smaller than the symbol size.<sup>34</sup> The lines are linear least-squares fit to the data.

solution increases accordingly, being essentially driven by the translational entropy of the “free” counterions. The progressive decrease of the scattering intensity at low scattering angles correlates well with the expected increase of the osmotic compressibility.

However, the most notable effect of the addition of acid is the appearance of a peak in the scattering profiles, which becomes sharper upon increasing  $\alpha$ . The presence of this peak is a common feature of polyelectrolyte solutions<sup>13,19,20</sup> and charged colloidal suspensions<sup>21</sup> and is consistent with the previous observations of charged dendrimers by Briber et al., Valachovic, and Ramzi et al.<sup>22–24</sup> This peak can originate both from a depletion of the scattering intensity due to the increased osmotic compressibility of the solution and also from the presence of a peak in the structure factor, indicating a preferential wavelength for spatial density–density fluctuations. In general, it is very difficult to separate unambiguously the  $P(q)$  and  $S(q)$  contributions to the overall scattering. There exist robust numerical methods to perform this task [Glatter], but they are still model dependent. The most reliable data can in principle be

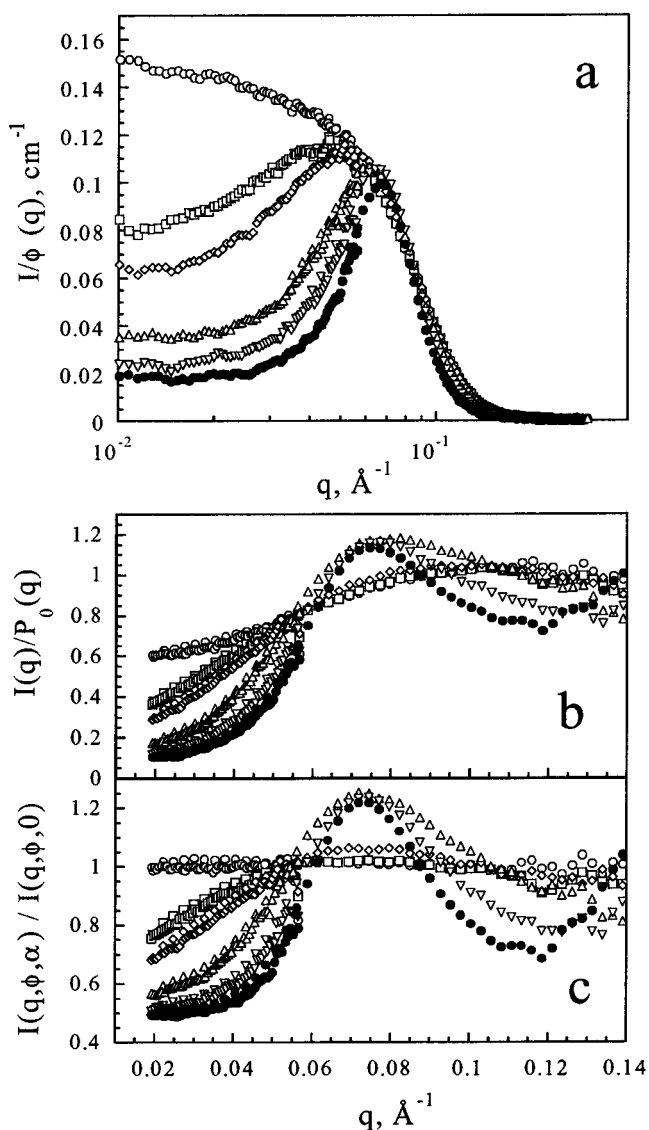


**Figure 3.** (a) Effect of the addition of HCl to the solutions of G5 PAMAM dendrimers with  $\phi = 0.042$ . Symbols correspond to  $\alpha = 0$  (open circles), 0.048 (squares), 0.072 (diamonds), 0.221 (triangles up), 0.449 (triangles down), and 0.960 (filled circles). (b) Plot of the scattering intensities divided by the form factor of the dendrimers extrapolated at zero concentration in the “uncharged conditions” (cf. Figure 2). (c) Plot of the scattering intensities normalized by the scattering profile of the dendrimer solution with  $\alpha = 0$  (cf. Figure 3a). The symbols are the same as in (a).

obtained experimentally, using zero-average contrast for instance,<sup>25</sup> but these experiments require deuterated samples, which are not always available.

In Figure 3b we plot the ratio of the scattering intensity and the form factor of the dendrimers extrapolated at zero concentration in the “uncharged conditions” (cf. Figure 1).<sup>26</sup> This is not a true “ $S(q)$ ” plot, as we cannot experimentally ascertain the effect of the charges on the form factor of the dendrimer in these experimental conditions. However, these data are consistent with a progressive onset of a preferential wavelength for spatial density–density fluctuations, as we note that the peak position is independent of the value of the charge parameter  $\alpha$ . Another way to represent the effect of increasing charge on the dendrimers, independent of a changing concentration, is to divide the total scattering intensity at each value of  $\alpha$  by the scattering from

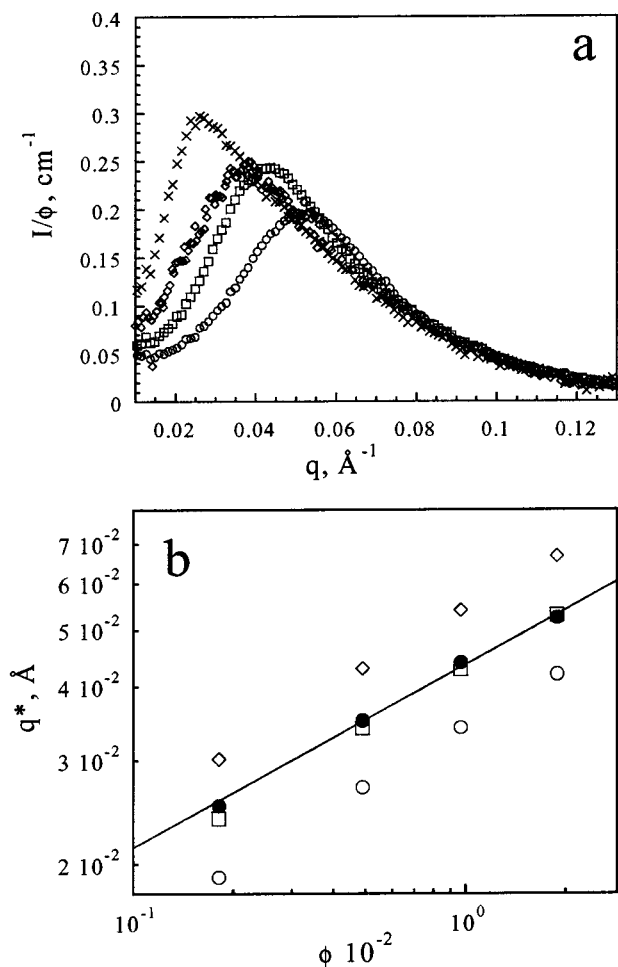


**Figure 4.** (a) Effect of dendrimer concentration on the scattering profiles for G5 PAMAM dendrimers with  $\alpha = 0.6$ . The scattering data are normalized by the dendrimer volume fractions of the solutions. Symbols represent  $\phi = 0.11$  (crosses), 0.31 (diamonds), 0.61 (squares), and 1.19 (circles). (b) Evolution of the peak position  $q^*$  as a function of dendrimer concentration (filled circles). The solid line is a power law fit to the data. For comparison, the expected results for the nearest-neighbor distance corresponding to simple cubic (circles), body-centered cubic (squares), and face-centered cubic (diamonds) packing for spheres with radius  $R = 31 \text{ \AA}$  are also shown.

the same finite concentration solution without added acid. This is shown in Figure 3c. Again, the peak position is independent of  $\alpha$  as is expected for a progressively more pronounced particle-particle spatial correlation.

Further insights into the origin of the peak in the scattering profile are given by evolution of the peak position with dendrimer volume fraction and added salt concentration. Figure 4 shows the variation of the scattering profiles as the dendrimer concentration increases, for  $\alpha = 0.6$ . A nonlinear least-squares fit to the data shows that  $q^*$  varies as  $\phi^\beta$  with  $\beta = 0.32 \pm 0.01$ .<sup>16</sup> The value of the scaling exponent is consistent with a simple volume expansion of the interparticle separation as the dendrimer concentration decreases. In solutions of linear polyelectrolytes in similar conditions  $q^*$  usually varies as  $\phi^\beta$  with  $\beta$  close to 0.5. For comparison, we also plotted the expected results for the nearest-neighbor distance corresponding to different regular packing of spheres having an equivalent radius  $R = 31 \text{ \AA}$ , which would correspond to a dense sphere profile of the dendrimers. Overall, the data clearly show that the peak

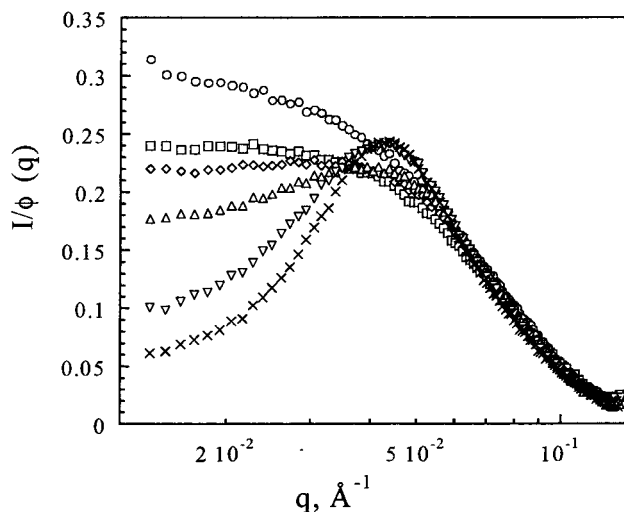


**Figure 5.** Effect of the addition of NaCl to charged dendrimer solutions with  $\alpha = 0$  and  $\phi = 0.04$ . Symbols correspond to  $C_S = 0$  (crosses), 5 mM (triangles down), 25 mM (triangles up), 50 mM (diamonds), 100 mM (squares), and 1000 mM (circles). Note that at 1 M of NaCl we recover the scattering profile of dendrimer solutions prior to addition of HCl.

position is related to the average interparticle distance and is indicative of a local liquidlike ordering of the macroions. It should also be mentioned that the average interparticle distances ( $\sim 2\pi/q^*$ ) range from 120 to 250  $\text{\AA}$  over the maximum concentration range in this study (cf. Figure 4b), which is considerably greater than the particle diameter, so that the origin of the scattering peak cannot be related to the swelling of the dendrimers. Therefore, the origin of this local ordering is not the volume excluded by neutral dendrimers in solutions, as observed at higher concentrations,<sup>15</sup> but is due to the presence of long-range interactions. As the charge on each dendrimer increases, electrostatic repulsions give rise to an effective electrostatic excluded volume,<sup>4</sup> resulting in an average distance of closest approach between the dendrimers.

The electrostatic origin of this liquidlike ordering can be further ascertained by considering the effect of salt on the scattering profiles, as dendrimer-dendrimer interactions ought to be screened by the addition of salt. This fact is illustrated in Figure 5, which shows that with the addition of NaCl we recover progressively the scattering profile characteristic of uncharged dendrimer solutions. The screening effect is not very surprising as it is a common feature of colloidal and polyelectrolyte solutions. However, Figure 5 also shows what is perhaps the most interesting feature of these dendrimer solutions, namely the fact that even at high salt concentrations, we do not observe the onset of attractive interactions, which would lead to an increase of the scattered intensity at low  $q$ .

Attempts to fit the data with a renormalized mean spherical approximation (RMSA) model<sup>27</sup> including a spherical approximation for the dendrimer form factor yielded unphysical results in most cases. It was possible to find reasonable fitting parameters in better agreement with the experimental data, but only by assuming size and shape (ellipticity) variations of the dendrimers which are not consistent with the quantities measured experimentally by SAXS. Even in these cases, the overall fitted charge density was on the order of 30%–50% of the charge parameter  $\alpha$ , which is consistent with previous comparisons between this model and experi-

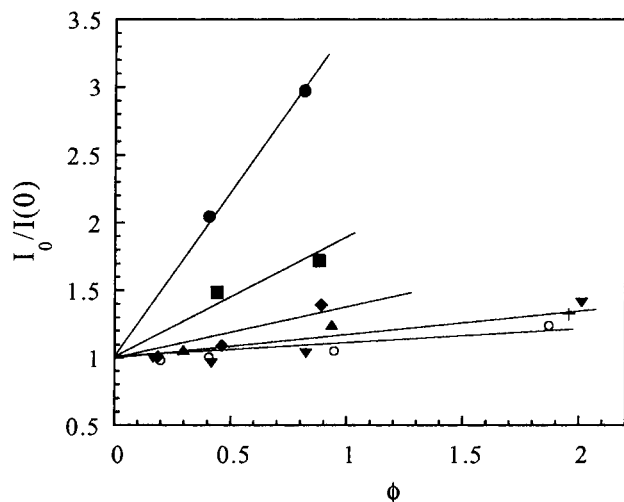


**Figure 6.** Inverse of  $I(0)$  as a function of dendrimer volume fraction ("Debye" plot). The data are normalized by the common intercept at  $\phi = 0$ ,  $I_0$ . Solid lines are linear fits to the data. Symbols correspond to samples with  $\alpha = 0.6$  and  $C_S = 5$  mM (filled circles), 25 mM (squares), 50 mM (diamonds), 100 mM (triangles up), 1000 mM (triangles down), and 2000 mM (cross). Note that the circles refer to data from dendrimer in pure  $D_2O$  ( $\alpha = 0$ , no added salt). The slopes correspond to the second virial coefficient; a positive slope indicates repulsive interactions.

mental data.<sup>28</sup> Measurements performed on solutions of higher generation dendrimer should yield unambiguous results, as it is possible to fit the data for the form factor more reliably using the higher order features<sup>3</sup> for the higher generation dendrimers as a check to constrain the fit parameters. One can also wonder whether dendrimers are not intrinsically different than the physical problem modeled by RMSA, namely charges are not evenly distributed on the surface of a sphere. Although the charges are likely to be located in a shell near the periphery of the molecule, dendrimers are not solid spheres with well-defined surfaces, even though they maintain a spherical symmetry as shown by Prosa et al.<sup>3</sup> They are molecules that can be permeated by the solvent, unlike most colloidal particles and proteins. In this way dendrimers express their polymer character as distinct from the comparison with a model colloid.

It is however possible to resort to a more classical treatment of the data. For instance, the intensity extrapolated at  $q = 0$ ,  $I(0)$ , can be related to the second virial coefficient by standard thermodynamic relationships.<sup>14</sup> The slope of a plot of  $\phi/I(0)$  vs  $\phi$  can be used to evaluate the nature of the interactions between molecules in solution. The  $I(0)$  values were obtained by extrapolating the low- $q$  scattering data points.<sup>29</sup> Figure 6 shows that, for all concentrations of salt studied and  $\alpha = 0.6$ , we obtain a positive slope for a range of dendrimer concentrations, suggesting that short-ranged repulsive interactions dominate under these conditions. The general behavior of solutions of charged dendrimers is illustrated in Figure 7.

These results are in stark contrast to the behavior observed in many charged colloids and polyelectrolytes, which tend to show attractive interactions upon the addition of salt, i.e., salting-out. It is also remarkable that systems most similar to dendrimers, at least in terms of size and shape, are proteins,<sup>30,31</sup> micelles,<sup>32</sup> and colloidal particles,<sup>33</sup> all of which display strong attractive interactions and would salt-out under comparable conditions. This study was limited to the effect of

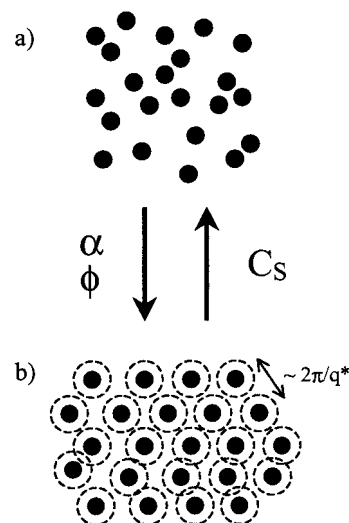


**Figure 7.** Illustration of the ordering phenomena observed in dendrimer solutions, represented by the filled circles. (a) Addition of salt screens the long-range electrostatic interactions and leads to a gaslike structure. The dotted circles in (b) represent the electrostatic excluded volume.

monovalent salts. It will be of interest to extend it to the case of multivalent salts.

## Conclusion

SANS measurements have been conducted on G5 PAMAM dendrimers in  $D_2O$  to determine their relevance as model polyelectrolytes and model colloids. We show that the dendrimers studied behave as noninteracting particles in dilute solutions in  $D_2O$  but that the addition of acid, which ionizes the dendrimers, induces a local ordering of the molecules in solution. Scattering from charged dendrimer solutions exhibits a peak that scales with the volume fraction with an exponent of  $0.32 \pm 0.01$ , indicating liquidlike ordering. The interactions can further be manipulated by the addition of monovalent salt to screen the electrostatic interactions. Extrapolations of the scattering data to  $q = 0$  yield the osmotic compressibility of the dendrimer solutions. For all the conditions studied, we find positive values of the second virial coefficients. We did not observe the onset of attractive interactions, even for the highest salt concentrations. This result is in stark contrast to most weak polyelectrolyte systems. The ensemble of results of this study suggests that PAMAM dendrimers are good candidates for model charged colloids since there is a large parameter space over which these solutions can be manipulated and measured.

**Acknowledgment.** We are especially grateful to D. Tomalia for providing the dendrimers, and we thank B. J. Bauer for many useful discussions. G. Nisato gratefully acknowledges the financial support by the Blancheflor Ludovisi-Boncompagni Foundation. This material is based upon work supported in part by the U.S. Army Research Office under Contract 35109-CH.

## References and Notes

- (1) Tomalia, D. A. *Science* **1991**, *252*, 1231.
- (2) Tomalia, D. A. *Sci. Am.* **1995**, *272*, 62.
- (3) Prosa, T. J.; Bauer, B. J.; Amis, E. J.; Tomalia, D. A.; Scherrenberg, R. *J. Polym. Sci., Part B: Polym. Phys.* **1997**, *35*, 2913.
- (4) Schmitz, K. S. *Macroions in Solution and Colloidal Suspension*; VCH Publishers: New York, 1993.

- (5) Certain commercial material and equipment are identified in this publication in order to specify adequately the experimental procedure. In no case does such identification imply recommendation by the National Institute of Standards and Technology nor does it imply that the material nor equipment identified is necessarily the best available for this purpose.
- (6) The parameters reported here were supplied by the manufacturer and were not measured at NIST.
- (7) Uppuluri, S.; Tomalia, D. A.; Dvornic, P. R. *ACS PMSE Prepr.* **1997**, *77*, 116.
- (8) The maximum total uncertainties can be estimated to be within 10% of the shown values.
- (9) Prask, H. J.; Rowe, M.; J., R. J.; Schroeder, I. G. *J. Res. Natl. Inst. Stand. Technol.* **1993**, *8*, 1.
- (10) SANS Data Reduction and Imaging Software, NIST-Cold Neutron Research Facility, 1996.
- (11) Glatter, O.; Kratky, O. *Small-Angle X-ray Scattering*; Academic Press: London, 1982.
- (12) Chen, S.-H., Bendedouch, D., Hirs, C. H. W., Timasheff, S. N., Eds. Academic Press: New York, 1986; Vol. 130, p 79.
- (13) Schosseler, F.; Moussaid, A.; Munch, J.-P.; Candau, S. J. *J. Phys. II* **1991**, *1*, 1197.
- (14) Higgins, J. S.; Benoit, H. C. *Polymers and Neutron Scattering*; Clarendon Press: Oxford, 1994.
- (15) Topp, A.; Bauer, B. J.; Amis, E. J., submitted to *Macromolecules*.
- (16) The uncertainty corresponding to one standard deviation is calculated from the fit parameters.
- (17) The accepted SI unit of concentration, mol/L, has been represented by the symbol M in order to conform to the conventions of this journal.
- (18) Swelling Response of PAMAM Dendrimers in Aqueous Solutions.
- (19) Ermi, B. D.; Amis, E. J. *Macromolecules* **1996**, *29*, 2701.
- (20) Ermi, B. D.; Amis, E. J. *Macromolecules* **1998**, *31*, 7378.
- (21) Arora, A. K.; Tata, B. V. R. *Ordering and Phase Transitions in Charged Colloids*; VCH Publishers: New York, 1996.
- (22) Briber, R. M.; Bauer, B. J.; Hammouda, B.; Tomalia, D. *Abstr. Pap.—Am. Chem. Soc.* **1992**, *204*, 225.
- (23) Structural Characterization and Polyelectrolyte Behavior of Poly(amido amine) Dendrimers Investigated by Light and Neutron Scattering Methods.
- (24) Ramzi, A.; Scherrenberg, R.; Brackman, J.; Joosten, J.; Mortensen, K. *Macromolecules* **1998**, *31*, 1621.
- (25) Cotton, J. P. *Adv. Colloid Interface Sci.* **1996**, *69*, 1.
- (26) The data were also normalized to take into account the effect of dendrimer concentration.
- (27) Hansen, J.-P.; Hayter, J. B. *Mol. Phys.* **1982**, *46*, 651.
- (28) Bendedouch, D.; Chen, S.-H. *J. Phys. Chem.* **1983**, *87*, 1473.
- (29) Since we cannot totally discard the influence of  $P(q)$  at low- $q$  vectors, we did not attempt to quantify the virial coefficients. However, the  $P(q)$  of the dendrimers is a constant, as shown in a forthcoming paper, so that the qualitative trend is correct.
- (30) Ducruix, A.; Guilloateau, J.-P.; Ries-Kraut, M.; Tardieu, A. *J. Cryst. Growth* **1996**, *168*, 28.
- (31) Velev, O. D.; Kaler, E. W.; Lenhoff, A. M. *Biophys. J.* **1998**, *75*, 2682.
- (32) Corti, M.; De Giorgio, V. *J. Phys. Chem.* **1981**, *85*, 711.
- (33) Arora, A. K.; Tata, B. V. R. *Ordering and Phase Transitions in Charged Colloids*; VCH: New York, 1996.
- (34) Uncertainty bars correspond to one standard deviation, calculated from the goodness of the fit.

MA990631H